J. of Electromagn. Waves and Appl., Vol. 23, 473–482, 2009

AN EFFICIENT PATTERN SYNTHESIS METHOD FOR CYLINDRICAL PHASED ARRAY ANTENNAS

Q.-Q. He, H.-D. He, and H. Lan

Southwest China Institute of Electronic Technology
Chengdu 610036, China

Abstract—An efficient approach for calculating the far field pattern of conformal phased array antennas mounted on cylindrical-shaped platforms is proposed. The array structure is taken into account by using an active element pattern technique, and the array is analyzed by using an element-by-element approach. The effects of all mutual couplings in the array environments are considered rigorously, and the efficiency of the proposed method is validated by using the commercial full-wave simulation software HFSS. Finally, a low side-lobe cylindrical phased array is designed for engineering by optimizing phases and amplitudes of port excitations.

1. INTRODUCTION

The process of choosing the parameters of an antenna array to produce desired radiation characteristics is known as pattern synthesis [1–3]. There are a wide variety of techniques that have been developed for the synthesis of linear and planar array [4–6]. The more complicated problem of synthesizing radiation patterns for conformal arrays on curved surfaces has been considered in recent years.

Because a conformal array is curved, new far field pattern behaviors emerge and many of the traditional linear and planar array synthesis methods are not valid. In [7], an iterative least-squares synthesis technique was presented for optimizing the element excitations and obtaining desired pattern shapes in conformal array. In [8, 9], the particle swarm optimization algorithms were applied to design low side-lobe patterns of conformal arrays. Jiao et al. [10] used a non-linear optimization technique to find a set of array coefficients that yield a pattern meeting a specified or a best attainable side-lobe

Corresponding author: Q.-Q. He (heqingqiang518@sohu.com).

level and achieving the maximum directivity. Furthermore, some other techniques such as intersection approach [11], simulated annealing technique [12], or adaptive array theory [13] can also be found in conformal array pattern synthesis. Recently, Wang et al. [14] presented the alternating projection method to optimize the weight vectors of conformal array antenna and obtained a good low cross-polarisation pattern. Unfortunately, these synthesis methods mentioned above are made to achieve favorable controls on the side-lobe level and beam shape, and they deal with relatively simple element pattern modeling. The element mutual couplings of conformal arrays are not considered rigorously.

In this paper, an efficient method for calculating radiation patterns of conformal array antennas is proposed. Starting from the analysis of mutual coupling between elements, an active element pattern technique [15] which considers the effects of all mutual couplings is given. Applying the principle of superposition, the far field radiated by a fully excited array is obtained. Based on optimizing phases and amplitudes of port excitations, a low side-lobe cylindrical phased array is effectively designed for engineering.

2. FORMULATION

Considering an N-element arbitrary array, each element in the array is modeled with independent generators, where the mnth element has an applied generator voltage and internal impedance given by V_{mn}^g and Z_{mn}^g. The voltage and current which include all coupling effects are V_{mn} and I_{mn}. At the terminals of each element, incident voltage and currents are V_{mn}^+ and I_{mn}^+, and reflected voltage and currents are V_{mn}^- and I_{mn}^-. Thus, the total terminal voltage and current at the mnth element are respectively

$$\begin{cases} V_{mn} = V_{mn}^+ + V_{mn}^- \\ I_{mn} = I_{mn}^+ - I_{mn}^- \end{cases} \tag{1}$$

Now consider the active element pattern of the mnth element, for which we set all voltage generators to zero except for the generator at the mnth element. An array of $M \times N$ elements is then treated as a $M \times N$ port network using Kirchhoff circuit theory analysis, giving

$$[V] = [Z][I] \tag{2}$$

where $[V]$ is a voltage column matrix of length $M \times N$, $[V] = [0, 0, \ldots, V_{mn}, \ldots, 0, 0]^T$, and the superscript "$T$" stands for the transpose operator. $[Z]$ is a impedance matrix; $Z_{mn,\,mn}$ is the self-impedance of the mnth element when all other elements are open

circuited; $Z_{mn,\,pq}$ is the mutual impedance between the two terminal pairs of elements mn and pq; and the mutual impedance $Z_{mn,\,pq}$ is the open circuit voltage produced at the first terminal pair divided by the current supplied to the second when all other terminals are open circuited. $[I]$ is a current column matrix of length $M \times N$, $[I] = [I_{mn,11},\, I_{mn,12},\, \ldots,\, I_{mn,\,pq},\, \ldots,\, I_{mn,\,MN}]^T$, and $I_{mn,\,pq}$ represents the current value at the pqth element when the mnth element is excited.

Solving (2) for $I_{mn,\,pq}$, we obtain

$$I_{mn,\,pq} = (-1)^{pq+1} V_{mn} \frac{|Z_{sl,\,jk}|_{sl \neq mn,\ \text{and}\ jk \neq pq}}{|Z_{sl,\,jk}|} \tag{3}$$

where $|Z_{sl,\,jk}|$ is determinantal operator. The active element pattern of the mnth element can be obtained as follows

$$\mathbf{F}^a_{mn}(\theta,\, \varphi) = \frac{1}{I_{mn,\,mn}} \sum_{pq=1}^{N_T} I_{mn,\,pq} \mathbf{F}^o_{pq}(\theta,\, \varphi) e^{jk\mathbf{r}_{pq}\cdot\hat{\mathbf{r}}} \tag{4}$$

where $\mathbf{F}^a_{mn}(\theta,\, \varphi)$ is the active element pattern of the mnth element; $\mathbf{F}^o_{pq}(\theta,\, \varphi)$ is the pattern of an isolated element; $e^{jk\mathbf{r}_{pq}\cdot\hat{\mathbf{r}}}$ is the spatial phase term; $\mathbf{r}_{pq}$ is a position vector from the origin to the center of the pqth element; $\hat{\mathbf{r}}$ is the unit radial vector from the coordinate origin in the observation direction $(\theta,\, \varphi)$; N_T is the element numbers of whole array and $N_T = M \times N$. Boldface type indicates a vector quantity.

Obviously, the expression of (4) indicates that the active element pattern is different from the isolated element pattern because other elements will radiate some power due to mutual coupling with the fed element. Furthermore, the active element pattern also depends on the position of the feed element, the characteristics of array element, and the geometry of the array.

By the principle of superposition, the far field radiated by a fully excited array can be expressed as follows

$$\mathbf{E}_{total}(\mathbf{r}) = \sum_{mn=1}^{N_T} I_{mn} \mathbf{F}^a_{mn}(\theta,\, \varphi) e^{jk\hat{\mathbf{r}}\cdot\mathbf{r}_{mn}} \tag{5}$$

In the fully excited phased array configuration, scanning to the direction of $\hat{\mathbf{r}}_0$ requires that the current at each element is phased as $a_{mn} e^{-jk\mathbf{r}_{mn}\cdot\hat{\mathbf{r}}_0}$, where a_{mn} is the current amplitude. The resulting field from the scanned array is then given by

$$\mathbf{E}_{total}(\mathbf{r}) = \sum_{mn=1}^{N_T} a_{mn} \mathbf{F}^a_{mn}(\theta,\, \varphi) e^{jk(\hat{\mathbf{r}}\cdot\mathbf{r}_{mn} - \hat{\mathbf{r}}_0\cdot\mathbf{r}_{mn})} \tag{6}$$

The analysis and design of most practical problems of conformal array antenna require extremely large computational domains, which leads to heavy computation burden [16, 17]. Owing to the limit of computer hardware, numerical techniques are relatively hard for the calculation of conformal array antennas when the number of array elements is enormous. Based on the analysis above, the array elements can be divided into edge, interior, and adjacent edge elements, where the adjacent edge elements locate between edge and interior elements. All elements are classified by their positions into three groups. For a particular excited element, i.e., the active element, the mutual coupling effects mainly come from its neighboring elements and the effects from far elements can be neglected. Thus, their active element patterns can be approximately calculated by substituting a small sub-array in their group for the whole array, and this reduces the computation burden remarkably. Therefore, the far field of (6) may be rewritten as

$$\mathbf{E}_{total}(\mathbf{r}) = \mathbf{E}_e(\mathbf{r}) + \mathbf{E}_i(\mathbf{r}) + \mathbf{E}_{ae}(\mathbf{r}) \tag{7}$$

where $\mathbf{E}_e$, $\mathbf{E}_i$, and $\mathbf{E}_{ae}$ are the superposition of the active element patterns of all edge, interior, and adjacent edge elements, respectively.

3. DESIGN AND DISCUSSION

Figure 1 shows the geometry of a finite and periodic array of $M \times N$ microstrip patches mounted on the surface of a dielectric coated circular cylinder with an outer radius b, inner radius a, dielectric thickness $h = b - a = 1.6\,\text{mm}$, and relative permittivity $\varepsilon_r = 4.4$. The back of the substrate is a cylindrical perfect conductor. A square patch with a length of $L = 0.39\lambda_0$ and width of $W = 0.33\lambda_0$ is selected as the radiating element, where λ_0 is the free space wavelength corresponding to an operating frequency of 3.1 GHz. Each patch is uniformly spaced from its neighbors by distances of D_z in the z-direction and D_φ in the φ-direction.

Figure 2 gives the isolated and active element patterns. It is clear that the isolated element pattern is different from the active element patterns because of the mutual coupling effects. The fact confirms the importance of analyzing the mutual coupling effects in this array environment.

Figure 3 plots the far field patterns for a $M \times N = 5 \times 5$ cylindrical array by using our proposed method and by the whole-array full-wave simulation, respectively. The chosen cylinder outer radius is $3\lambda_0$ and spacing between elements is $0.8\lambda_0$. From Fig. 3, we can see that the results from our method are consistent with those of whole-array full-wave simulation when the 5×5 cylindrical array is fully excited.

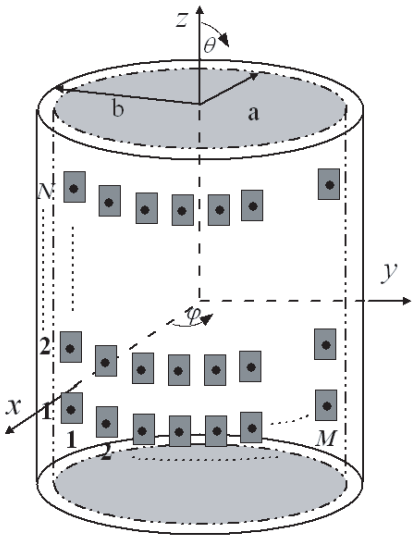

Figure 1. Geometry of the cylindrical microstrip array.

Furthermore, Fig. 3 also reveals that the curvature plays a significant role for the side-lobe level of the cylindrical array pattern. The first side-lobe starts to merge with the main beam and a concave-shape appears in the main radiating direction. Therefore, the phases of port excitations must be compensated for the cylindrical array to avoid the high side-lobe level, and the corresponding compensated values can be given by

$$\Delta\phi_n = \frac{2\pi}{\lambda_0}\mathbf{R}_n \cdot \hat{r}_0 \tag{8}$$

where $\hat{r}_0$ is the unit vector in the direction of the main-beam peak (θ_0, φ_0).

Through compensating the phases of port excitations, the far field pattern of the cylindrical phased array is similar to that of classical planar array; the main-beam becomes narrow and the side-lobe level descends. Of course, for certain applications, the amplitudes of port excitations also need to be modified in order to obtain lower side-lobe level. The excited amplitude a_{mn} of the mnth element is obtained as

$$a_{mn} = \frac{T_{mn}S_{mn}}{F_{mn,\max}(\theta_0, \varphi_0)} \tag{9}$$

where T_{mn} is the value of the desired distribution function at the projected of the mnth element on the aperture plane; S_{mn} is the

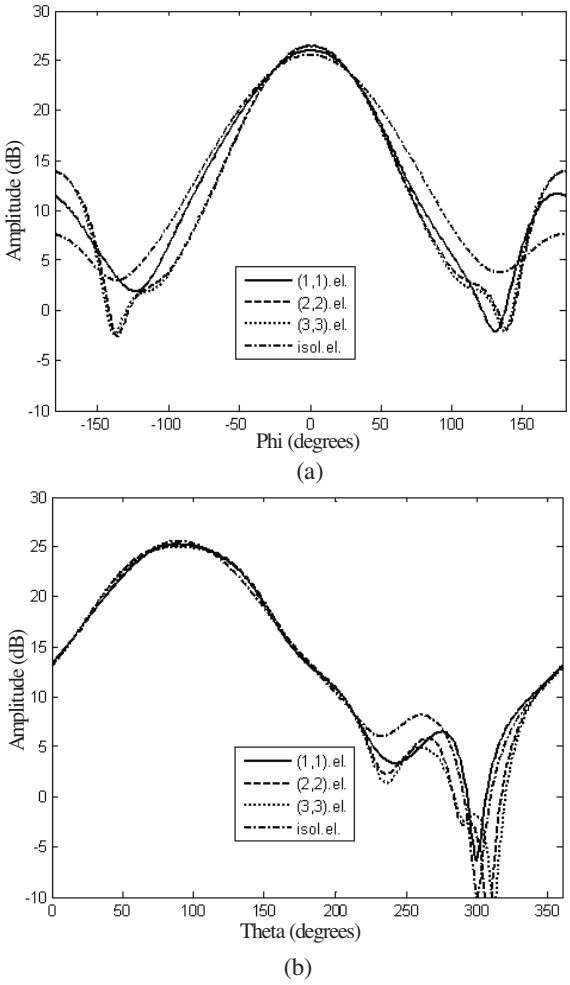

Figure 2. Calculated active element pattern for different array elements in a 5×5 array, compared to the radiation pattern of an isolated element, (a) xoy-plane and (b) xoz-plane.

projected area occupied by the mnth element; and $F_{mn,\max}$ is the amplitude of the element pattern in the main beam direction.

Figure 4 gives the synthesized beams of the cylindrical phased array by compensating the phases and optimizing the amplitudes of port excitations. Here, T_{mn} uses a 40 dB Taylor weights for a 10×10 element array. It is obvious that the side-lobe level is consistent with the ideal level of -40 dB in the 0° scan direction. When beam steers

to 30° off boresight, the beamwidth is slightly wider and the side-lobe level is slightly higher. But the low side-lobe level is still maintained and satisfies the demand for engineering. Unlike the original design concept of Dubost, applying 40 dB Taylor weights to the conformal array results in only −27 dB side-lobe level [18].

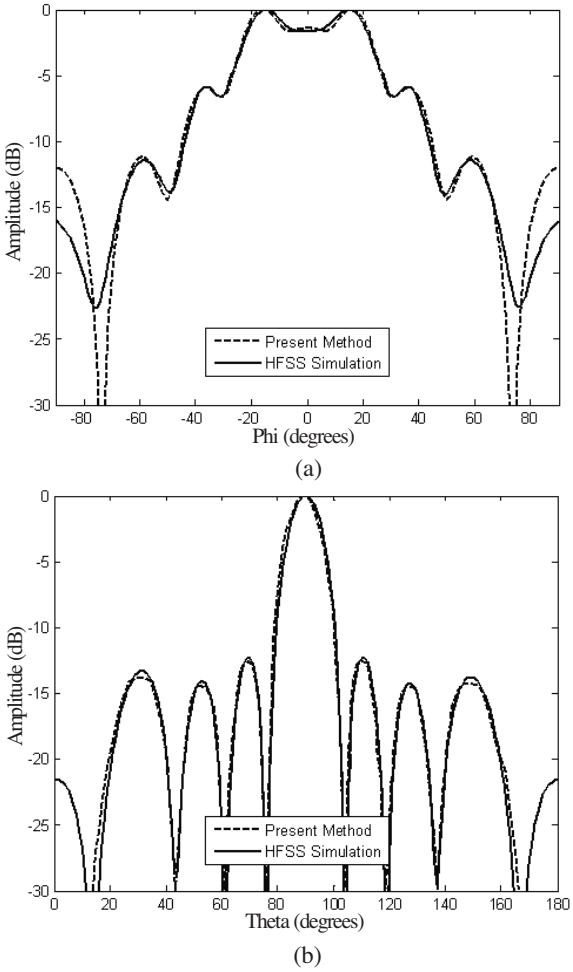

Figure 3. Far field patterns for the 5×5 cylindrical array with equal amplitude and cophasal excitations, (a) xoy-plane and (b) xoz-plane.

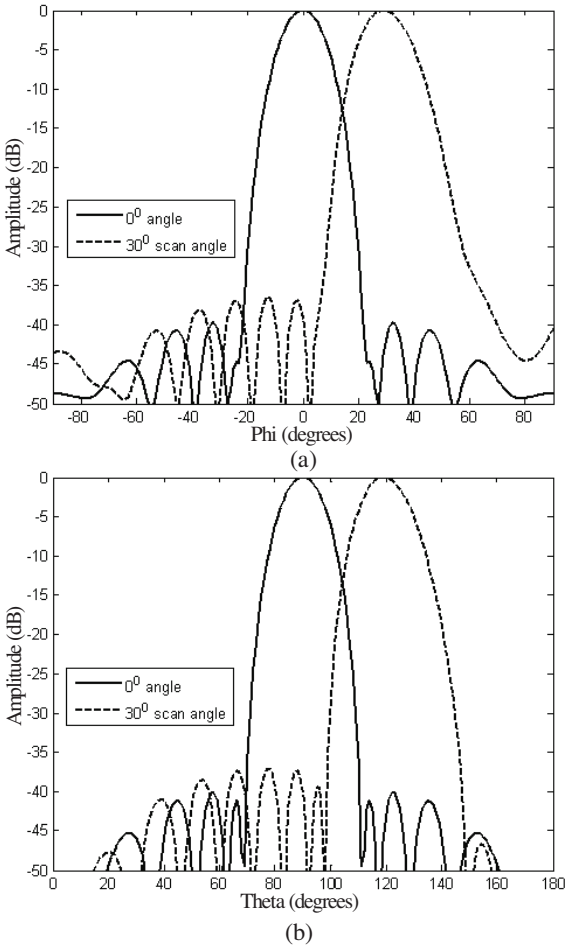

Figure 4. Far field patterns for the 10×10 cylindrical phased array with a half-wavelength element spacing, (a) xoy-plane and (b) xoz-plane.

4. CONCLUSION

In this paper, an efficient method based on the active element pattern technique for calculating the far field patterns of cylindrical phased array antennas is proposed. The theoretical model, in which the effects of all mutual couplings in the array environment are considered rigorously, is given. In order to validate the proposed method, a 5×5 cylindrical array is studied, and the results show that our method

is valid and efficient for calculating the far field patterns. Based on the proposed method, a low side-lobe cylindrical phased array is synthesized. The synthesis technique yields the sets of excited current phases required to compensate as much as possible for platform effects and excited current amplitudes required to meet a low side-lobe level.

REFERENCES

1. Liu, X. F., Y. C. Jiao, and F. S. Zhang, "Conformal array antenna design using modified particle swarm optimization," *Journal of Electromagnetic Waves and Applications*, Vol. 22, No. 2–3, 207–208, 2008.
2. Oraizi, H. and M. T. Noghani, "Design and optimization of nonuniformly spaced longitudinal slot arrays," *Progress In Electromagnetics Research M*, Vol. 4, 155–165, 2008.
3. Azevedo, J. A. R., "Shaped beam pattern synthesis with non-uniform sample phases," *Progress In Electromagnetics Research B*, Vol. 5, 77–90, 2008.
4. Mahanti, G. K., A. Chakrabarty, and S. Das, "Phased-only and amplitude-phase only synthesis of dual-beam pattern linear antenna arrays using floating-point genetic algorithms," *Progress In Electromagnetics Research*, PIER 68, 247–259, 2007.
5. Rocca, P., L. Manica, and A. Massa, "Directivity optimization in planar sub-arrayed monopulse antenna," *Progress In Electromagnetics Research Letters*, Vol. 4, 1–7, 2008.
6. Qu, Y., G. Liao, S.-Q. Zhu, and X.-Y. Liu, "Pattern synthesis of planar antenna array via convex optimization for airborne forward looking radar," *Progress In Electromagnetics Research*, PIER 84, 1–10, 2008.
7. Vaskelainen, L. I., "Iterative least-squares synthesis methods for conformal array antennas with optimized polarization and frequency properties," *IEEE Trans. Antenna Propagat.*, Vol. 45, No. 7, 1179–1185, July 1997.
8. Lu, Z. B., A. Zhang, and X. Y. Hou, "Pattern synthesis of cylindrical conformal array by the modified particle swarm optimization algorithm," *Progress In Electromagnetics Research*, PIER 79, 415–426, 2008.
9. Boeringer, D. W. and D. H. Werner, "Bézier representations for the multiobjective optimization of conformal array amplitude weights," *IEEE Trans. Antenna Propagat.*, Vol. 54, No. 7, 1964–1970, July 2006.
10. Jiao, Y.-C., W.-Y. Wei, L.-W. Huang, and H.-S. Wu, "A new low

side-lobe pattern synthesis technique for conformal arrays," *IEEE Trans. Antenna Propagat.*, Vol. 41, No. 6, 824–831, June 1993.

11. Mazzarella, G. and G. Panarieello, "Pattern synthesis of conformal arrays," *IEEE AP-S Int. Symp.*, 1054–1057, 1993.
12. Ferrira, J. A. and F. Ares, "Pattern synthesis of conformal arrays by the simulated annealing technique," *Electron. Lett.*, Vol. 33, No. 14, 1187–1189, July 1997.
13. Zhou, P. Y. and M. A. Ingram, "Pattern synthesis for arbitrary array using an adaptive array method," *IEEE Trans. Antenna Propagat.*, Vol. 47, No. 5, 862–869, May 1999.
14. Wang, B.-H., Y. Guo, Y.-L. Wang, and Y.-Z. Lin, "Frequency-invariant pattern synthesis of conformal array antenna with low cross-polarisation," *IET Microw. Antennas Propag.*, Vol. 2, No. 5, 442–450, August 2008.
15. Pozar, D. M., "The active element pattern," *IEEE Trans. Antenna Propagat.*, Vol. 42, No. 8, 1176–1178, August 1994.
16. Raffaelli, S., Z. Sipus, and P.-S. Kildal, "Analysis and measurements of conformal patch array antennas on multilayer circular cylinder," *IEEE Trans. Antenna Propagat.*, Vol. 53, No. 3, 1105–1113, Mar. 2005.
17. He, Q.-Q. and B.-Z. Wang, "Radiation pattern synthesis for a conformal dipole antenna array," *Progress In Electromagnetics Research*, PIER 76, 327–340, 2007.
18. Dubost, G., "Wideband flat dipole and short-circuit microstrip patch elements and array," *Handbook of Microstrip Antennas*, J. R. James and P. S. Hall (eds.), Peter Peregrinus Ltd, 1989.